https://dx.doi.org/10.22161/ijaers.74.8 *ISSN: 2349-6495(P) | 2456-1908(O)*

Influence of plastic deformation over the natural frequency of steel structures

Ana C. C. Barbosa, Rodrigo R. F. Pinto, Janes Landre Jr.

Department of Mechanical Engineering, Pontifícia Universidade Católica de Minas Gerais, Belo Horizonte, Brazil

Abstract*— *The modal analysis is an important step during the project of structures. Throughout it, it is possible to know structural properties that may help when it is necessary to analyze the integrity of the system. Many studies and researches are being developed to understand more deeply the phenoms that involve mechanical vibrations, especially because of their importance. One of these phenoms, for example, crucial in aeroelasticity, is the flutter, that requires the coupling of two different natural frequencies, which may happen when the material is plastically deformed. In its turn, the coupling requires the variation of natural frequencies, which was experimentally observed by this work through traction tests and modal analysis.

Keywords*— *Modal analysis, Natural frequencies, Plastic deformation.

I. INTRODUCTION

The modal analysis aims to determine the dynamic parameters of a system. Through it, it is possible to know indispensable properties to analyze the integrity of structures and machines when exposed to a specific boundary condition, such as fluid-structure interaction. It also helps to design solutions that enhance the reliability and security of the structure when under critical operation conditions, such as alternating loads capable of inducing resonance conditions [1]. One of the most famous cases of resonance is the Tacoma Bridge, that exhibited big oscillations before collapsing on November 7th, 1940. Those displacements were caused by the interaction between the wind and the structure [2].

Another phenom capable of causing failures and breakage of structures in aeroelasticity is the flutter. In typical wings, it happens when the air condition induces a decrease of the equivalent damping factor of the system and the natural frequencies of bending and torsion are coupled, causing unstable oscillations. Thus, flutter in typical wings demands not only a specific atmosphere condition but a convergence of natural frequencies [3].

Therefore, natural frequencies and mode shapes are directly related and must be analyzed during the design process, especially when dynamic loads are imposed on the system. Depending on the nature of the boundary condition, such as the atmosphere, the material properties, and the geometry, a different dynamic response may be observed, and that must be predicted in the project phase.

II. NATURAL FREQUENCY AND DEFORMATION

The natural frequencies of a system with *n* degrees of freedom may be determined by the calculation of the eigenvalue of its motion equation that may be modeled through the Lagrange equation:

$$\frac{d}{dt}\left(\frac{\partial T}{\partial \dot{x}_i}\right) - \frac{\partial T}{\partial x_i} + \frac{\partial V}{\partial x_i} = F_i \qquad (1)$$

in which $\boldsymbol{F_i}$ is a non-conservative force, $\boldsymbol{T}$ is the kinetic energy and $\boldsymbol{V}$ is the potential energy of the system.

In turn, the energies $\boldsymbol{T}$ and $\boldsymbol{V}$ may be written as:

$$T = \frac{1}{2} M v^2 \qquad (2)$$

$$V = \frac{1}{2} K x^2 \qquad (3)$$

in which $\boldsymbol{v}$ is the velocity, $\boldsymbol{x}$ is the displacement, $\boldsymbol{M}$ is the mass and $\boldsymbol{K}$ is the stiffness.

Using numerical methods, it is possible to write the result of the substitution of (i.e., (3) and (i.e., (4) into (i.e., (1) in the matrix form below:

$$[M]\ddot{\vec{x}} + [K]\vec{x} = \vec{F} \qquad (4)$$

https://dx.doi.org/10.22161/ijaers.74.8 *ISSN: 2349-6495(P) | 2456-1908(O)*

Assuming a conservative system, (i.e., (4) turns into a homogeneous differential equation which solution adopts the format:

$$T(t) = C_1 \cos(\omega t + \phi) \qquad (5)$$

in which C_1 is the amplitude and ϕ is the phase of the movement. This solution shows that all the coordinates may move harmonically at the same frequency ω and in the same phase ϕ.

But the frequency ω may not assume any arbitrary value. Since this equation may be written as a system of equations of *n* degrees of freedom, the trivial solution is zero. However, for the other solutions, the coefficient matrix must be zero, making this an eigenvalue problem and resulting in a polynomial equation which roots are *n* values of ω^2, where ω^2 is the eigenvalue and ω is the natural frequency of the system. Thus, the natural frequency may be expressed as:

$$\omega_n^2[M]\vec{X}^{(n)} = [K]\vec{X}^{(n)} \qquad (6)$$

As presented by (i.e., (6), the natural frequency ω is a function of the stiffness matrix $[K]$ and the mass matrix $[M]$.

Similarly, it is possible to write the torsion natural frequency as:

$$\omega_{t_n}^2[J]\vec{X}^{(n)} = [K_t]\vec{X}^{(n)} \qquad (7)$$

in which $[K_t]$ is the torsional stiffness matrix and $[J]$ is the polar mass moment of inertia matrix.

One of the most powerful methods to estimate natural frequencies is the Finite Element. It is based on the discretization of the analyzed system and provides great flexibility to understand the dynamic responses of a structure when submitted to different boundary conditions in a virtual environment. However, the preliminary results of a Finite Element analysis differ from the reality, and Experimental or Operational Modal Analysis are constantly required to adjust the virtual model to the reality. These distortions may have many causes, such as joint conditions, discrepancies in material geometry and nonlinearity [4].

Therefore, comprehending the mathematics behind the natural frequencies modes is important to investigate if any properties of the system are capable of leading to natural frequency variation. Since the mass is not likely to vary under standard operation conditions, the variation must come from the resultant stiffness. The tensile test is one of the procedures utilized to determine and study the properties of a material, and its main output is the Stress-Strain curve [5].

The Stress-Strain curve has two well-defined regions. The first one is the elastic region, where the strain and the stress of the material presents a linear behavior expressed mathematically by the Hooke's Law:

$$\sigma = E\varepsilon \qquad (8)$$

in which σ is the stress, ε is the deformation and E is the Young modulus, which expresses the material resistance to deformation.

The second is the plastic region, where the strain and the stress have a non-linear dependency. Many equations define this region, but one of the most commonly used is the Hollomon's Law:

$$\sigma = Y\varepsilon^n \qquad (9)$$

in which Y is the tensile strength coefficient and n is the strain hardening coefficient.

It is possible to transform the Strain-Stress curve in the elastic interval into a Force-Displacement curve applying the stiffness equation, which leads to the following form:

$$F = Kx \qquad [10]$$

The (i.e., (10) reinforces from another perspective that the stiffness of the material is constant in all the elastic region, and so, it must not be a parameter capable of inducing a variation of the natural frequency. However, if the material enters the plastic deformation, the stiffness is likely to vary because of the non-linear behavior expressed by the (i.e., (9).

Since the material assumes a non-linear dependency in the plastic region, it is not possible to apply Classical Mechanics to input and study its impacts in the movement equation and consequently in the natural frequency of the system. However, the Lagrangian Mechanics presents tools to solve this issue.

In 1992, Nogueira and Loeffler [6] added the non-linear properties model into Hamilton's Principle and studied the influence of multiple boundary conditions in the dynamic responses of beams via the Finite Elements Method (FEM).

https://dx.doi.org/10.22161/ijaers.74.8 *ISSN: 2349-6495(P) | 2456-1908(O)*

Hamilton's Principle consists of an integration in time and space that can be used to evaluate dynamic effects in structures when approached from the perspective of minimum potential energy. So, introducing the non-conservative effects of a system, it is possible to write the equation:

$$\int_{t_1}^{t_2}(\partial T + \partial W_e + \partial W_u + \partial W_a)dt = 0 \qquad (11)$$

in which ∂T is the variation of the kinetic energy of the structure; ∂W_e is the external virtual work; ∂W_u is the internal virtual work and ∂W_a is the virtual work of the dissipative forces.

After introducing the non-linear mathematic model of materials in each term of the (i.e., (11) and some simplifications, it is possible to write the global matrix equation of the movement:

$$[M]\ddot{x} + [C]\dot{x} + \vec{R} = f \qquad (12)$$

in which f is the external load, $[M]$ is the mass matrix of the structure, $[C]$ is the damping matrix of the structure and $\vec{R}$ is the stiffness vector.

As presented by Nogueira and Loeffler in (i.e., (12), the addition of non-linear properties into Hamilton's Principle prevents the emergence of the constant stiffness matrix $[K]$ as presented in (i.e., (4). In its place, however, appears the vector $\vec{R}$, which is a function of the stress and the deformation.

In one of the exercises, considering a beam subjected to followers loads, the authors identified that the plasticization of the material not only amplified the displacement but also increased the natural frequency. This survey is intended to go deeper into these observations, validate the prediction of natural frequencies variation in the simulated environment and verify this phenomenon through tensile tests.

III. TENSILE TEST AND MECHANICAL PROPERTIES

Since the main activity of the study was to perform an impact test during a tensile test, it was necessary to manufacture proof bodies specially designed for this application. For that, hot-rolled SAE 1020 steel was chosen because of the specifications and easy access.

The proof bodies were designed to attend the tensile test machine specifications and the standard ABNT NBR ISO 6892-1:2013. The rupture region had 10mm of diameter and 100mm of length, and the clamping region had 16mm of diameter. The total length was 302mm. One of the extremities was designed to be longer than the other, making it possible to mill an area and positioning the accelerometer. The manufacturing drawing is presented in Fig. 1.

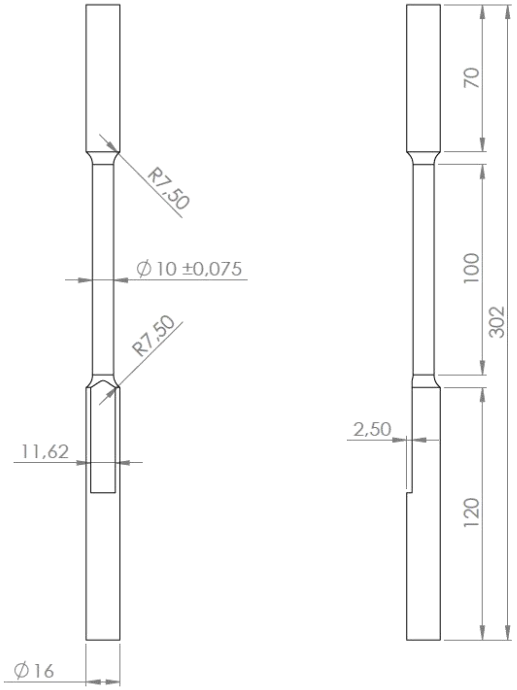

Fig. 1: Drawing of the proof bodies.

After the manufacturing of the proof bodies, two initial tensile tests were performed to obtain the stress-strain curve and determine the mechanical properties of the material and the system. The tensile machine utilized was the Emic GR048. An extensometer was utilized to determine the mechanical properties of the material, as presented in Fig. 2.

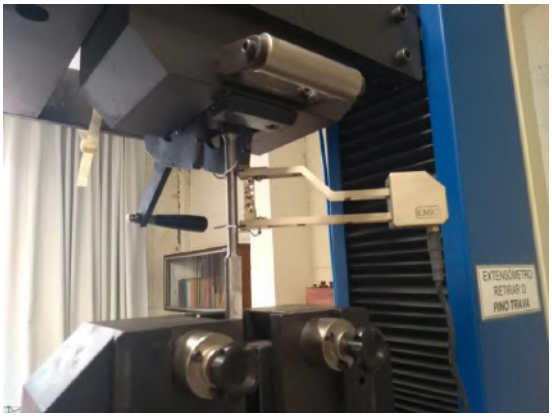

Fig. 2: Configuration of the mechanical properties tensile test.

https://dx.doi.org/10.22161/ijaers.74.8 *ISSN: 2349-6495(P) | 2456-1908(O)*

After the tests, the tensile test machine generated the stress-strain curves in Fig. 3 and calculated the Young module, the yield stress, and the maximum stress. The tensile strength and the strain hardening coefficient were calculated by the regression method adjusted to Hollomon's law as presented in Fig. 4.

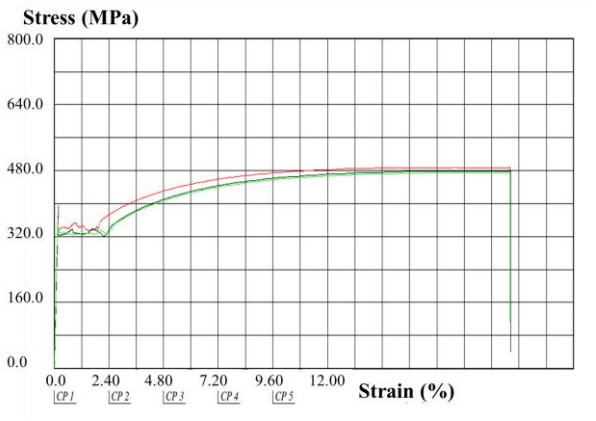

Fig. 3: Strain-stress curve generated by the tensile stress machine.

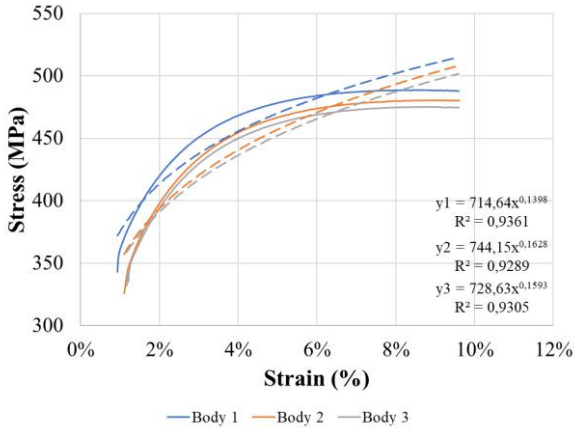

Fig. 4: Nonlinear regression with power adjustment utilized to determine the tensile strength and the strain hardening coefficient in the plastic region.

Table 1 presents a summary of the mechanical properties of the material.

Table 1: Mechanical properties of the material.

Property	PB01	PB02	PB03	Mean
Young Modulus [GPa]	199.5	219.1	220.4	213.0
Yield Stress [MPa]	343.1	325.0	329.5	332.5
Maximum Stress [MPa]	491.7	483.2	476.6	483.8
Tensile Strength Coef.	714.6	744.2	728.6	729.1
Strain Hardening Coef.	0.139	0.163	0.159	0.154

After the determination of the mechanical properties of the material, the other three tensile tests were performed to observe the system behavior. In these tests, the extensometer was not utilized, so the collected data refer to the system. The curves obtained are presented in Fig. 5.

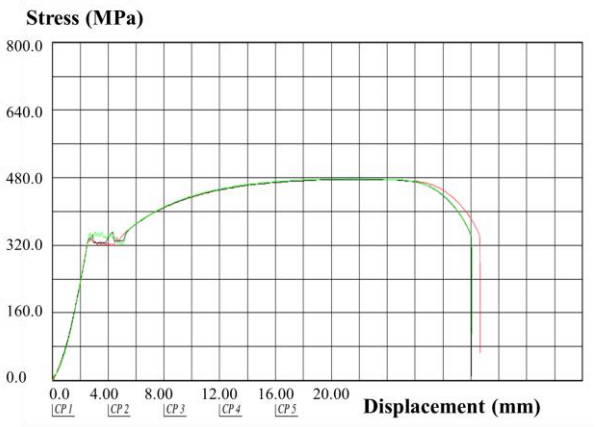

Fig. 5: Displacement-stress curve of the system.

From these curves, it was possible to calculate the mechanical properties of the system. The report generated by the machine provided the yield and the maximum stress, so it is possible to define the boundary of the elastic and plastic regimes.

Since the test was performed without the extensometer, it's not possible to measure the strain of the material. However, it is possible to measure the displacement of the machine and calculate properties analogous to Hook and Hollomon's laws. Thus, the Young module becomes the Elastic Resistance, the Tensile Strength Coefficient becomes a Plastic Resistance Coefficient and the Strain Hardening Coefficient remains as a Strain Hardening Coefficient. Performing this mathematical arrangement, it is possible to determine the values of each variable by regression methods adjusted to Hook and Hollomon's law as presented in Fig. 6. Table 2 presents a summary of the mechanical properties of the system.

https://dx.doi.org/10.22161/ijaers.74.8 *ISSN: 2349-6495(P) | 2456-1908(O)*

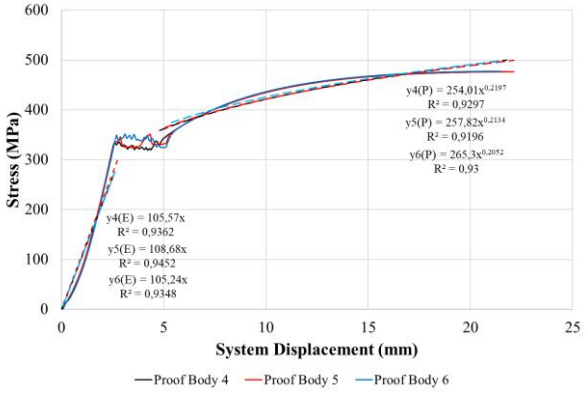

Fig. 6: Determination of the mechanical properties of the system.

Table 2: Mechanical properties of the material.

Property	PB04	PB05	PB06	Mean
Elastic Resist. [MPa/mm]	105.6	108.7	105.2	106.5
Yield Stress [MPa]	330.7	336.7	339.4	335.6
Maximum Stress [MPa]	476.7	476.4	477.9	477.0
Plastic Resistance Coef.	254.0	257.8	265.3	259.0
Strain Hardening Coef.	0.220	0.213	0.205	0.213

IV. FINITE ELEMENT MODELING

In order to validate the prediction of natural frequencies variation and define a range of frequencies to elaborate the Fast Impact Hammer Test (FIHT) presented in item 5, a modal analysis was performed using the free student software ANSYS Mechanical, which is a mechanical engineering software solution that uses finite element analysis (FEA) to solve structural engineering problems. A tension specimen was projected according to the standard ABNT NBR ISO 6892-1 and its geometry was modeled in ANSYS SpaceClaim interface, as presented in Fig. 7.

Since the subject of this survey is to study the natural frequency behavior of the system in both the elastic and plastic regions, linear analysis was not adequate for this simulation due to the non-linear properties of the material in the plastic region, so a non-linear analysis was required.

To elaborate a non-linear analysis in ANSYS Mechanical, the material Stress-Strain curve was obtained by a tensile test aiming approximate the material properties of the simulation to that used in the practice. The data was processed using (i.e., (8) and (i.e., (9) and imported to the software. Fig. 8 presents the curve imputed.

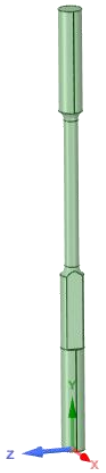

Fig. 7: Geometry of the tension specimen modeled in ANSYS SpaceClaim.

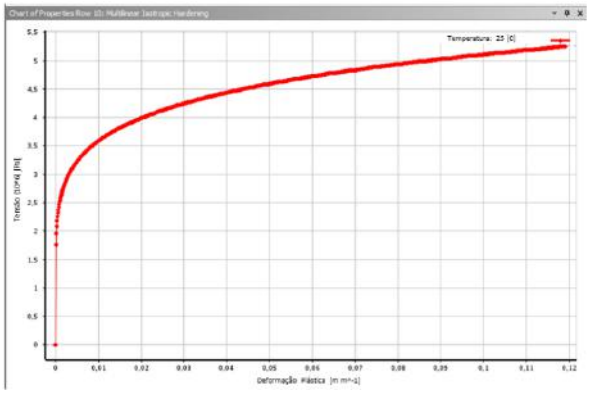

Fig. 8: Stress-Strain curve of the material imported to the software.

The modal analysis was elaborated considering a pre-stress condition based on a static structural analysis. The first test of mesh was performed considering a mesh of 1.5 mm, which led to an extremely refined model. For this reason, tests using other dimensions were performed and it was possible the attribution of a mesh ten times less refined with just 2% of variation in results. Since this magnitude of variation is not significant considering the purpose of the simulation, the default mesh was attributed.

Besides that, it was necessary to stipulate contour conditions to the static analysis to reproduce the behavior of a tensile test. Therefore, a fixed support was applied to the underside of the specimen's model, while a displacement was applied on the upper side.

The displacement condition has been configured to allow translation along the Y axis but restrict movement along the X and Z axes. Fig. 9 shows these configurations applied to the model.

https://dx.doi.org/10.22161/ijaers.74.8 ISSN: 2349-6495(P) | 2456-1908(O)

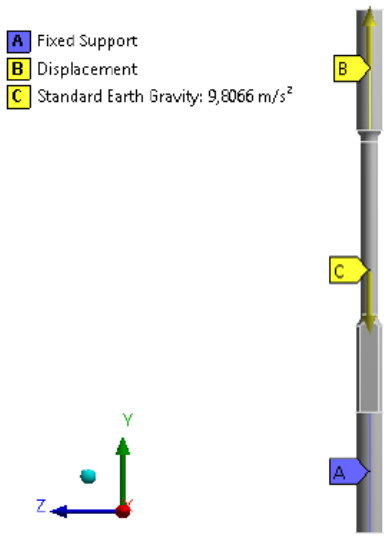

Fig. 9: Contour conditions established to the tension specimen's model.

The static analysis was performed considering displacements from 0 to 9.5 mm. To each displacement applied, a modal analysis with pre-stress was elaborated and the first natural mode was noted in order to build a Frequency x Strain curve. The results obtained are presented in Table 3 and the curve constructed is shown in Fig. 10.

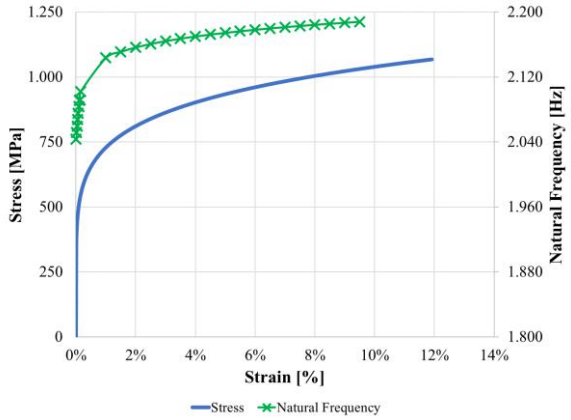

Fig. 10: Frequency x Strain curve elaborated considering the modal analysis performed.

Table 3: Modal analysis results by using the Finite Element Method.

Displacement [mm]	Frequency [Hz]
0.00	2,043.7
0.02	2,051.7
0.04	2,059.7
0.06	2,067.7
0.08	2,075.6
0.10	2,083.5
0.12	2,091.2
0.14	2,091.7
0.16	2,102.3
1.00	2,143.6
1.50	2,151.1
2.00	2,156.5
2.50	2,160.8
3.00	2,164.3
3.50	2,167.4
4.00	2,170.0
4.50	2,172.4
5.00	2,174.5
5.50	2,176.5
6.00	2,178.3
6.50	2,180.0
7.00	2,181.5
7.50	2,183.0
8.00	2,184.4
8.50	2,185.7
9.00	2,186.9
9.50	2,188.1

V. TENSILE AND IMPACT TESTING

After the simulations in virtual environment, the tensile test was performed along with the impact test. The accelerometer was set in the lower extremity of the proof body, in the milled area. The setting of the experiment is presented in Fig. 11. The strain-stress curve of the system was utilized to determine frequency measurement points, as presented in Fig. 12.

https://dx.doi.org/10.22161/ijaers.74.8 *ISSN: 2349-6495(P) | 2456-1908(O)*

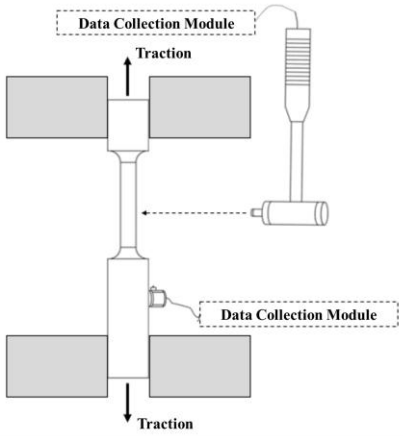

Fig. 11: Setting of the tensile-impact test.

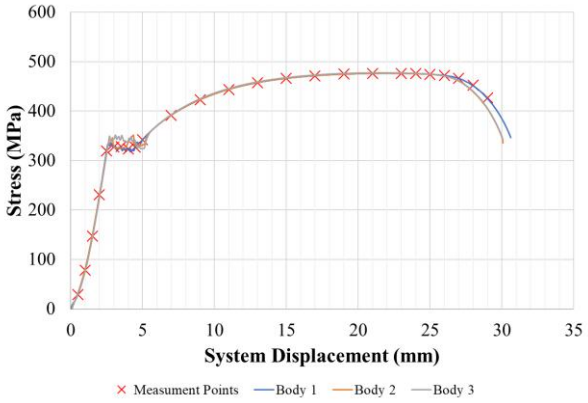

Fig. 12: Natural frequency measurement points along the Stress-Strain curve of the system.

To attend the natural frequencies estimated by the simulation, the operating manual of the hammer was utilized to select the hard tip (80 lbf pk) to perform the impact test. The acceleration was measured by the accelerometer and the collection module. The software CatMan Easy was utilized to perform the Fast Fourier Transform and determine the natural frequency of the system. Fig. 13 presents examples of the data collected.

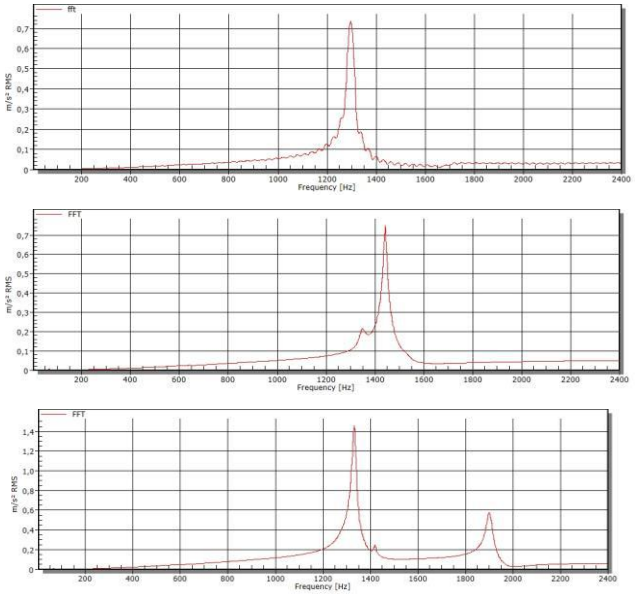

Fig. 13: FFT of the natural frequency measurement in a) 0.5mm; b) 4.0mm; and c) 23.0mm of displacement.

The natural frequencies obtained in function of the displacement are summarized in Table 4, and Fig. 14presents it graphically.

Table 4: Natural frequencies measurements by proof body and displacement of the system.

Displacement [mm]	Natural Frequency PB01 [Hz]	Natural Frequency PB02 [Hz]	Natural Frequency PB03 [Hz]
0.5	-	1,209	1,296
1.0	-	1,267	1,345
1.5	-	1,320	1,387
2.0	-	-	1,426
2.5	1,429	1,395	1,463
3.0	-	1,398	1,452
3.5	-	1,392	1,446
4.0	-	1,386	1,442
4.5	1,413	1,382	1,437
5.0	1,409	1,380	1,434
7.0	1,404	1,379	1,430
9.0	1,395	1,372	1,421
11.0	1,383	1,361	1,412
13.0	1,366	1,349	1,399
15.0	1,353	1,332	1,384

https://dx.doi.org/10.22161/ijaers.74.8 *ISSN: 2349-6495(P) | 2456-1908(O)*

17.0	1,337	1,321	1,371
19.0	1,322	1,300	1,358
21.0	1,305	1,284	1,344
23.0	1,290	1,273	1,332
24.0	1,281	-	1,332
25.0	-	1,262	1,320
26.0	1,271	-	1,320
27.0	-	1,250	1,320
28.0	1,259	-	1,320
29.0	1,246	1,239	1,293

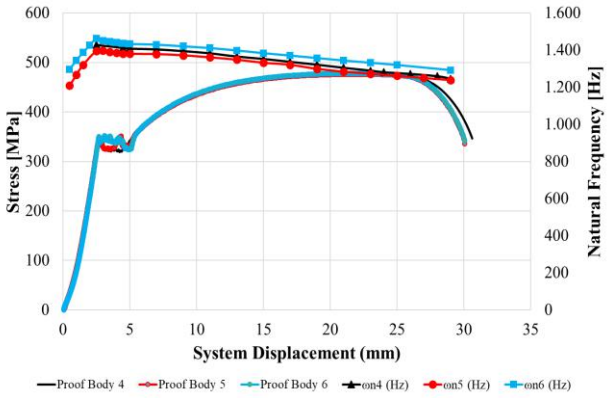

Fig. 14: Experimental natural frequency and Stress vs System Displacement.

VI. CONCLUSION

Focusing on the experimental data collected, it was possible to construct the graphic Stress and Natural Frequency vs Strain presented in Fig. 15. From that, it was possible to observe that the natural frequency of a system varies according to the state of stress and deformation. In the elastic regime, a significant positive statistical correlation was obtained, validating the tendency of increasing frequency due to the increase in deformation. In addition, it was found that the variation of the natural frequency in this regime adopts a linear profile with an average variation of 89 Hz/mm displaced.

Similar behavior was observed in the plastic regime. In this case, it was possible to perceive a high negative statistical correlation, proving a tendency for the natural frequency to reduce due to the increase in deformation. In this regime, it was also possible to observe a linear behavior whose average variation is approximately -6 Hz/mm displaced.

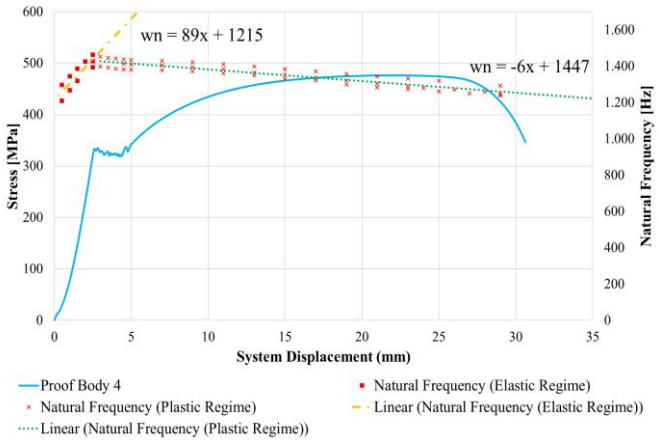

Fig. 15: Stress and Natural Frequencies vs Strain.

Before analyzing the collected data, it was necessary to treat them mathematically so that they were on the same basis. Since the simulated natural frequencies in Table 3 is a function of the strain, it was necessary to transform it into a function of the system displacement. However, there is no mathematic function that transforms the displacement of the system into the deformation caused in the test region of the material, especially because of lots of phenoms such as slippings and the deformation of the clamping extremities happens during the tensile test. Despite that, it was possible to observe that the behavior of the curves from the simulation and the experimental tests are not similar.

From Fig. 10, it was possible to observe that the static simulation indicates a tendency of growth of the natural frequency of the system as it deforms, being the growth stronger during the elastic regime and weaker in the plastic regime. The same behavior was not observed in the experimental data collected and presented in Fig. 14, that shows a tendency of growth of the natural frequency in the elastic regime and a tendency of reduction in the plastic regime.

Such conclusions allow perceiving that a static-equivalent simulation similar to the one carried out in this work does not adequately the behavior of the material in the elaborated experiment. In addition, for greater assertiveness of results, it is necessary to use the data obtained empirically in the experiments to determine the main characteristics of the boundary condition of the system and, based on this, develop another simulation that is closer to the real condition of the test.

REFERENCES

[1] Harris, Cyril M. and Piersol, Allan G. Harris' Shock and Vibration Handbook. 6. s.l.: McGraw Hill, 2009.

https://dx.doi.org/10.22161/ijaers.74.8 *ISSN: 2349-6495(P) | 2456-1908(O)*

[2] Rao, Singiresu S. Mechanical Vibrations. 5th. s.l.: Pearson, 2010.
[3] Mukherjee, Somenath and Arvind, BG. A Theoretical Formulation for Flutter Analysis of a Typical Subsonic Aircraft Wing (SARAS) Using Quasi-Steady Aerodynamic Theory. Bangalore: NAL, 2005.
[4] Mohanty, Prasenjit. Operational Modal Analysis in the Presence of Harmonic Excitations. Balasore: Indian Institute of Technology, 2005.
[5] Callister, William D. and Rethwisch, David G. Materials Science and Engineering: An Introduction. s.l.: John Wiley & Sons, 2009.
[6] Nogueira, José Carlos and Loeffler, Carlos Friedrich. Análise Elasto-Plástica de Estruturas Planas Submetidas a Cargas Móveis. [book auth.] Congresso Ibero Latino-Americano Sobre Métodos Computacionais para a Engenharia. Anais. Porto Alegre: s.n., 1992, pp. 107-116.